Rev. Roum. Sci. Techn.– Électrotechn. et Énerg.
Vol. **62**, *2*, pp. 129–133, Bucarest, 2017

PERFORMANCE COMPARISON OF VOLTAGE SAG/SWELL DETECTION METHODS IMPLEMENTED IN CUSTOM POWER DEVICES

MEHMET BÜYÜK, MUSTAFA İNCİ, MEHMET TÜMAY

Key words: Sag/swell detection, Improved synchronous reference frame (SRF), Second order generalized integrator phase locked loop (SOGI-PLL), Enhanced phase locked loop (EPLL), Fast Fourier transform (FFT).

In distribution systems, voltage sag/swell is known as the most hazardous disturbances which distort voltage stability in sensitive loads. In order to compensate these voltage disturbances via custom power devices, fast and accuracy detection of voltage sag/swell is the most significant issue for effective compensation. Therefore, this paper aims to examine and compare detection capabilities of the most common sag/swell detection methods. In this study, EPLL, SOGI-PLL, FFT and ISRF are assessed among the detection methods. The common point of these methods is that they are applicable for both three-phase system and single-phase system as well. The performances of proposed methods are analyzed and compared for both single phase sag/swell condition and three-phase asymmetrical sag/swell conditions. The methods are compared through constructing sag/swell generation system in PSCAD/EMTDC.

1. INTRODUCTION

Recently, the importance of electrical power quality has been increasing in the industrial world due to increase in demand for electric energy and consisting of sensitive electric loads. Voltage sag and voltage swell are the well-known disturbances among power quality problems in distribution systems [1]. Voltage sag and swell conditions are demonstrated in Fig. 1. Voltage sag is defined as reduction in rms value of voltage magnitude more than 0.1 pu (per unit). Besides, voltage swell is short duration rise in magnitude more than 0.1 pu [2, 3]. The duration of voltage sag/swell varies from half-period to 1 minute which is defined in IEEE 1159–2009 standards [4, 5]. In order to compensate these problems, custom power devices based on power electronic systems are developed [6–10]. Custom power devices (CPDs) are power-electronics based devices used in distribution systems to provide stable voltage level for consumers [11, 12]. In the system, the grid voltage is firstly measured, and the magnitude of the voltage is determined via a detection method to obtain reference signal. This reference signal is used to produce the desired voltage level by switching the inverter switching components. Thus, voltage sag/swell is compensated, and the voltage level at the load side is maintained in level of standards.

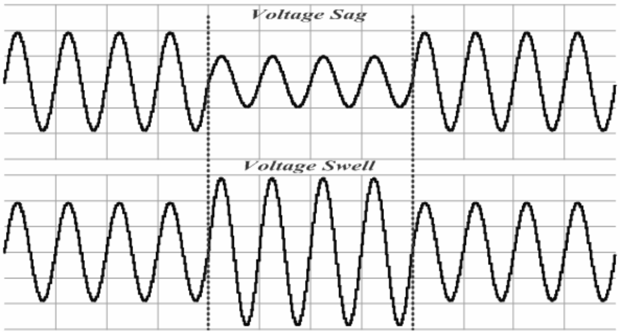

Fig. 1 – Voltage sag/swell conditions in electrical grids.

Fast and accurate detection of sag/swell is significant subject for effective compensation [4, 13, 14]. There are several sag/swell detection methods to obtain magnitude information of voltage signals. Therefore, this paper aims to examine and compare capabilities of several sag/swell detection methods. In this study,

- Enhanced phase locked loop (EPLL) [15, 16],
- Second order generalized integrator phase locked loop (SOGI-PLL) [17],
- Fast Fourier transform (FFT) [18, 19] and
- Improved synchronous reference frame (ISRF) [7]

methods are assessed among the detection methods.

The common point of these methods is that they are applicable for three-phase system and single-phase system as well. The performances of the four methods are compared for three-phase asymmetrical sag and three-phase asymmetrical swell conditions. The methods are compared through constructing sag/swell generation system in PSCAD/EMTDC.

2. SYSTEM CONFIGURATION AND DETECTION METHODS

Figure 2 illustrates system configuration to compensate sag/swell problems. In system, CPDs are located between sensitive load and grid to compensate voltage sag/swell by injecting controlled voltage. In compensation process, voltage signals are initially measured and converted to per unit (pu) values. Then, these values are used as inputs (V_a ,V_b and V_c) in detection method to acquire the amplitude of voltage signals in pu. During sag/swell situation, the voltage magnitude is subtracted from nominal value (1 pu) to generate the depth of voltage sag/swell. Then, obtained value is processed in controller to produce reference value of injected voltage via CPDs.

Sag/swell detection method plays an important role for effective compensation. In order to realize effective compensation, voltage sag/swell must be detected fast and properly. In literature, there are several sag/swell detection methods which have different detection performance capabilities.

Electrical and Electronics Engineering, Çukurova University, Balcalı, 01330, Sarıçam, Adana, Turkey, E-mail: mbuyuk@cu.edu.tr, minci@cu.edu.tr, mtumay@cu.edu.tr

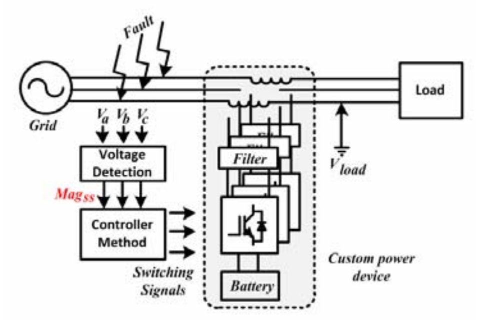

Fig. 2 – The system configuration.

In this study, four detection methods are taken into account, which can be applied for both three-phase system and single-phase system. The investigated methods are EPLL, SOGI-PLL, FFT and ISRF which generate magnitude information of grid voltages (Mag $_{SS}$).The voltage signals are tested in per unit system, and voltage sag/swell is detected according to (1), (2):

$$\text{Mag}_{SS} \le 0.9 \text{ pu for sag condition} \quad (1)$$

$$\text{Mag}_{SS} \ge 1.1 \text{ pu for swell condition.} \quad (2)$$

2.1. ENHANCED PHASE LOCKED LOOP

EPLL is a non-linear adaptive filter in terms of its structure, which can generate from the input signal its magnitude, phase and frequency. The block diagram of EPLL is shown in Fig. 3. EPLL is able to get the fundamental component of its input that contains power quality problems [16, 20]. Besides, it is not affected from other disturbances [15]. EPLL consists of phase detection (PD), low pass filter (LPF) and voltage controlled oscillator (VCO).

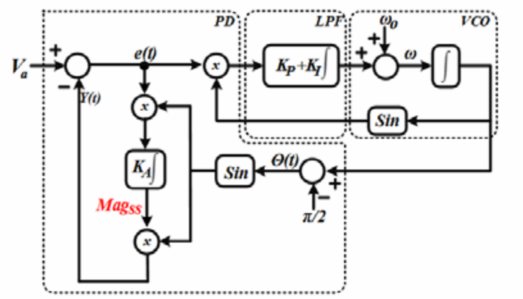

Fig. 3 – EPLL structure based sag/swell detection scheme.

The sag/swell is detected via getting magnitude of the input signal which is given in (3).

$$\text{Mag}_{SS} = \int e(t)\,\sin\theta(t)\,K_A\,\text{d}t\,. \quad (3)$$

And the error and phase angle equations are obtained from its block diagram as

$$e\,(t) = V_a\,(t) - \sin\theta(t) \int e(t) \sin\theta(t) K_A \text{d}t\,, \quad (4)$$

$$\theta\,(t) = -\pi/2 + \int [e\,(t) \cos\theta(t) K_P + \Delta\omega t + \omega_0]\,\text{d}t\,, \quad (5)$$

$$\Delta\omega t = \int e\,(t) \sin(\theta + \pi/2)(t) K i\text{d}t. \quad (6)$$

The error signal is the total distortion in input signal defined in time-domain as (4), where K_A, K_I and K_P are gains and integral constants which affect determination of magnitude and phase of the input signal. Thus, the speed and performance of EPLL are determined by these parameters [21].

2.2. SECOND ORDER GENERALIZED INTEGRATOR PLL

SOGI-PLL is a phase locked-loop which can be applied in both single phase and three phase systems. In addition to obtain phase information of a signal, it achieves the generation of amplitude of measured signal. It can also extract the amplitudes of asymmetrical voltage signals due to implementation for each phase, separately.

Electrical signals are usually distorted by harmonics. Adaptive filters are better way in order to be avoided from the harmonics since they are not affected too much from the harmonic characteristics and automatically adapt their parameters according to harmonic characteristics [17]. They are also applicable under three-phase asymmetrical conditions [22].

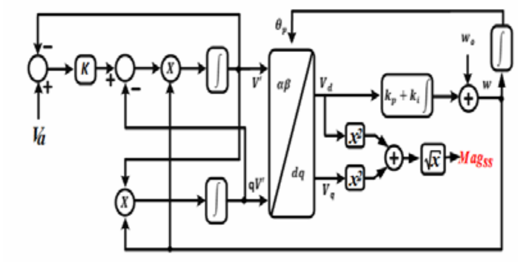

Fig. 4 – SOGI-PLL based sag/swell detection method.

According to scheme presented in Fig. 4, the characteristic functions can be derived as:

$$\text{SOGI}\ (s) = \frac{V'}{K}(s) = \frac{\omega' s}{s^2 + \omega}, \quad (7)$$

$$D_{\text{SOGI}}\ (s) = \frac{V'}{V}(s) = \frac{K\omega' s}{s^2 + K\omega' s + \omega^2}, \quad (8)$$

$$Q_{\text{SOGI}}\ (s) = \frac{qV'}{V}(s) = \frac{K\omega'^2}{s^2 + K\omega' s + \omega^2}, \quad (9)$$

$$\angle D_{\text{SOGI}} = \tan^{-1}\left(\frac{\omega'^2 - \omega^2}{K\omega'\omega}\right), \quad (10)$$

$$\angle Q_{\text{SOGI}} = \tan^{-1}\left(\frac{-K\omega'\omega}{\omega'^2 - \omega^2}\right), \quad (11)$$

$$\angle Q_{\text{SOGI}} = \angle D_{\text{SOGI}} - \pi/2\,. \quad (12)$$

Considering the output signals of SOGI-PLL, it produces two orthogonal signals which has 90° difference between two signals. By using these signals, the amplitude is calculated as the square root of sum of square of orthogonal signals. The magnitude signal is expressed as:

$$\text{Mag}_{SS} = \sqrt{V_d^2 + V_q^2}\,. \quad (13)$$

2.3. IMPROVED SRF

Conventional SRF theory cannot achieve detection of single phase or asymmetrical voltage signals [23–25]. In order to eliminate the drawback of this method, Improved SRF is introduced in this study to extract the amplitude signal of single phase and three phase signals. Improved SRF is an advanced method of SRF that is constructed by only single-phase signal instead of three-phase signals. Thus, the method becomes suitable for both single-phase systems and three-phase asymmetrical systems. The block diagram of ISRF is shown in Fig. 5.

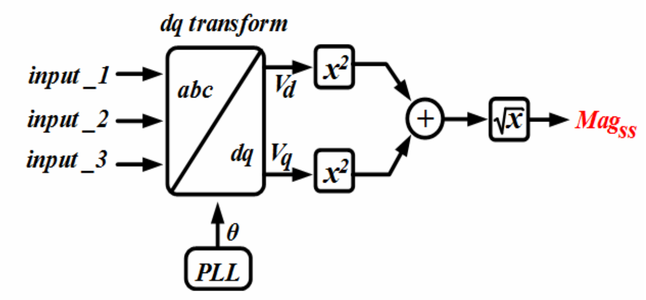

Fig. 5 – Improved SRF based sag/swell detection method.

In this method, each phase signal is separately evaluated as three-phase. According to d–q transform, there-phase symmetrical voltage signals are derived [26]. Because of symmetrical system, *input*_2 and *input*_3 can be rewritten in phasor form as (14) and (15). *input*_2 is delayed π/3 and multiplied with –1 which becomes same as 240° phase difference. In three-phase symmetrical systems, the sum of the voltages is zero. Therefore, *input*_3 becomes as (15).

$$input\_2 = V_a\angle\left(\frac{2\pi}{3}\right) = V_a\angle\left(\frac{4\pi}{3}\right) = \\ = V_a\angle(\pi)\times 1\angle\left(\frac{\pi}{3}\right) = -V_a\angle\left(\frac{\pi}{3}\right), \tag{14}$$

$$input\_3 = -(input\_1 + input\_2) = -V_a + V_a\angle\left(\frac{\pi}{3}\right). \tag{15}$$

In d–q transform process of controller method as shown, *input*_1, *input*_2 and *input*_3 are firstly converted to α and β components for single phase:

$$\begin{bmatrix} V_\alpha \\ V_\beta \end{bmatrix} = \sqrt{\frac{2}{3}} \begin{bmatrix} 1 & -\frac{1}{2} & -\frac{1}{2} \\ 0 & \frac{\sqrt{3}}{2} & -\frac{\sqrt{3}}{2} \end{bmatrix} \cdot \begin{bmatrix} V_a \\ -V_a\angle(\pi/3) \\ -V_a + V_a\angle(\pi/3) \end{bmatrix} . \tag{16}$$

Then, α–β to d–q transform is realized in (7).

$$\begin{bmatrix} V_d \\ V_q \end{bmatrix} = \begin{bmatrix} \cos(\omega t) & \sin(\omega t) \\ -\sin(\omega t) & \cos(\omega t) \end{bmatrix} \cdot \begin{bmatrix} V_\alpha \\ V_\beta \end{bmatrix}, \tag{17}$$

where ω is angular frequency and *t* is time in seconds. V_d and V_q are orthogonal signals. Therefore, the magnitude of the voltage is obtained by using d–q components as:

$$\mathrm{Mag}_{\mathrm{SS}} = \sqrt{V_d^2 + V_q^2} . \tag{18}$$

2.4. FAST FOURIER TRANSFORM

Fast Fourier transform (FFT) is a factorized process of DFT which results in using less complex computation [18]. Cooley-Tukey algorithm is the most common applied algorithm, which divides DFT into smaller DFT pieces as shown in Fig. 6 [19, 27]. FFT can generate dc component, fundamental frequency component and multiples of fundamental frequency component. In this study, only the magnitude of fundamental component is generated so as to get sag/swell of voltage. The Cooley-Tukey algorithm is explained in [28] in detail

$$V[k] = \underbrace{\sum_{n=0}^{\frac{N}{2}-1} v(2n) W_{\frac{N}{2}}^{nk}}_{V_{even}(k)} + W^k \underbrace{\sum_{n=0}^{\frac{N}{2}-1} v(2n+1) W_{\frac{N}{2}}^{nk}}_{V_{odd}(k)} , \tag{19}$$

where k is harmonic frequency index, N is number of samples and $W_k = e^{-\mathrm{j}2\pi k/N}$. $\mathrm{Mag}_{\mathrm{SS}}$ is calculated for $k = 1$

$$\mathrm{Mag}_{\mathrm{ss}} = V[1] = \underbrace{\sum_{n=0}^{\frac{N}{2}-1} v(2n) W_{\frac{N}{2}}^{n}}_{V_{even}(1)} + W^k \underbrace{\sum_{n=0}^{\frac{N}{2}-1} v(2n+1) W_{\frac{N}{2}}^{n}}_{V_{odd}(1)} . \tag{20}$$

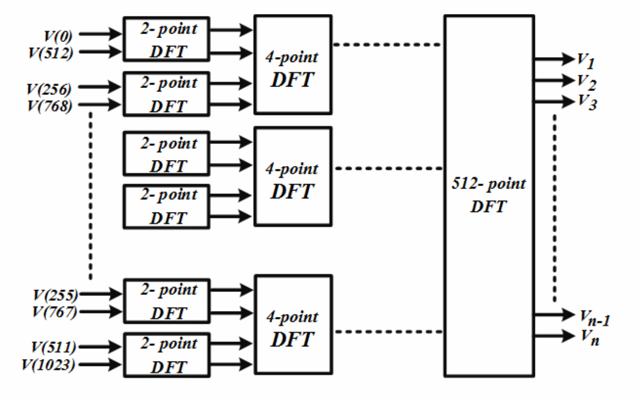

Fig. 6 – FFT based sag/swell detection method.

3. RESULTS AND DISCUSSION

The performances of the four sag/swell detection methods are compared for single phase sag/swell and three-phase asymmetrical sag/swell situations. In order to compare the performances, a single phase/three-phase system is constructed in PSCAD, as demonstrated in Fig. 2. The system consists of three-phase grid, three-phase RL load and a sag/swell generator. The sag/swell generator is used to fulfill sag and swell cases. It is placed between the grid and the load. The system parameters of modeling are given in Table 1.

Firstly, voltage detection methods are performed for a single phase system. Sag situation starts at 0.6 seconds, and voltage decreases to 0.4 pu from 1 pu during 0.1 seconds. Then, voltage signal returns to its steady-state value. At 0.8 seconds, the magnitude of voltage increases to 1.3 pu from 1 pu for 6 periods. The performance study is realized using four different methods to detect voltage disturbances. Performance results of voltage detection for Case I are presented in Fig. 7.

Table 1

System parameters

	Parameters	Value
Grid	Voltage	0.38 kV (1 pu)
	Frequency	50 Hz
PSCAD	Duration of run	2000 ms
	Solution time	0.02 ms
	Channel plot step	0.02 ms

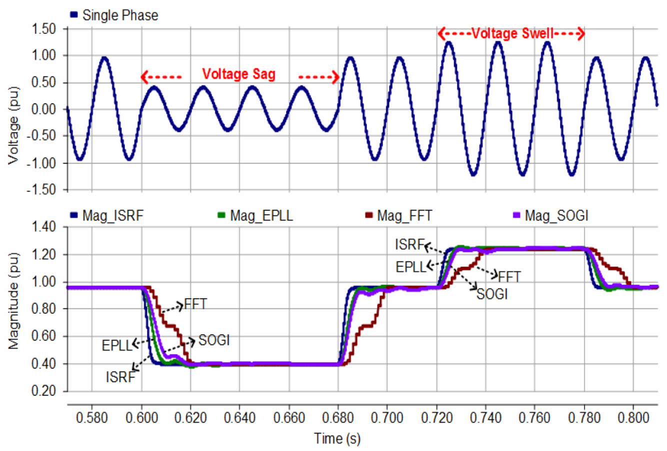

Fig. 7 – Performance results for Case I.

In the second case, performance results of asymmetrical voltage sag and asymmetrical voltage swell are tested for a three phase system. In this condition, voltage sag occurs between 0.9 and 0.96 seconds for 3-cycles. The values of three-phase asymmetrical voltage sag for V_a, V_b and V_c are 35 %, 25 % and 50 %, respectively. Also, three-phase asymmetrical voltage swell condition occurs between 1.04 and 1.1 seconds. The asymmetrical voltage swells for three phase (V_a, V_b and V_c) occur 25 %, 50 % and 40 %, respectively. The simulation results of Case II are presented in Fig. 8.

It can be seen from Fig. 7 and Fig. 8 that the performance of ISRF method is superior to the other three methods in detection of sag and swell cases. ISRF detects asymmetrical three-phase sag and asymmetrical three-phase swell with lower time delay compared with the other methods. The detection times of ISRF for 35 %, 25 % and 50 % sags are 1.9 ms, 0.6 ms and 1.1 ms, respectively. Besides, the detection times for 25 %, 50 % and 40 % swells are 1.7 ms, 0.6 ms and 0.4 ms, respectively.

FFT method is the worst method among the four methods to detect sag and swell. It is too slow compared with the other methods. Table 2 presents the features of voltage detection methods according to detection time advantages and disadvantages.

Table 2

Features of voltage detection methods

Method	Detection	Advantages	Disadvantages
EPLL	≈2 ms (0.1 period)	*Extra no phase information	*more oscillation *Mathematical complexity
SOGI-PLL	≈3 ms (0.15 period)	*Extra no phase information	*more oscillation *Mathematical complexity
ISRF	≈1 ms (0.05 period)	*Fast detection *Simple *Less oscillation	*Needs a phase information
FFT	≈6 ms (0.3 period)	*Less oscillation	*Needs a phase information *More slow

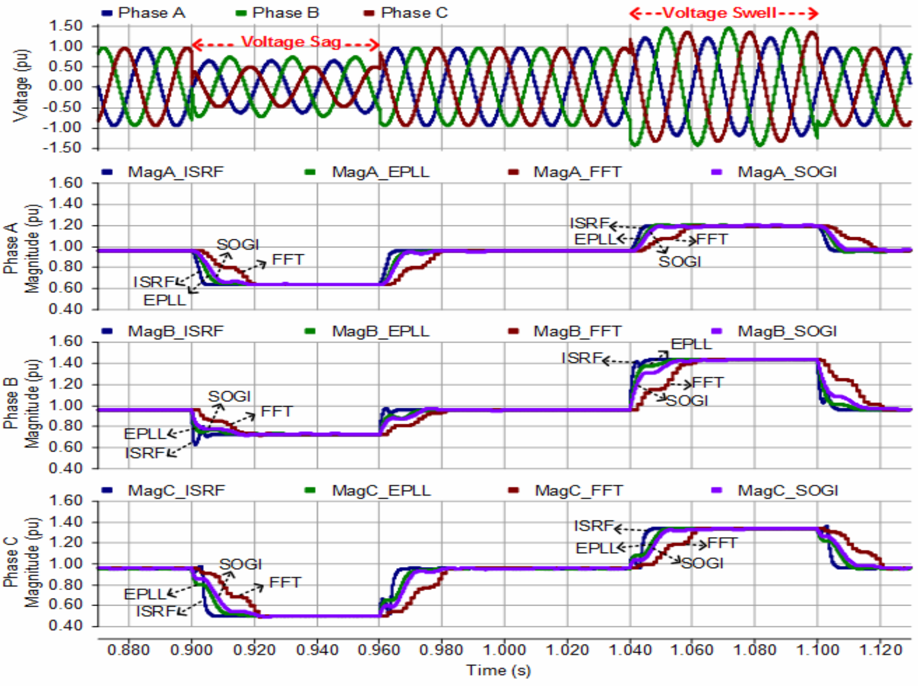

Fig. 8 – Performance results for Case II.

4. **CONCLUSIONS**

In the present paper, the performance comparison of four sag/swell detection methods has carried out. The common trait for the four methods is that they can be applied for both single-phase and three-phase systems. The performances of the methods are compared for three-phase asymmetrical sag and three-phase asymmetrical swell cases. Among the four methods, ISRF shows better robustness and faster detection time for sag and swell cases. In contrasts, FFT method is the slower one among the methods.

ACKNOWLEDGEMENTS

This work was supported by TÜBİTAK (Project Number: 115R304).

Received on March 19, 2016

REFERENCES

1. G.A.D. Carlos, E.C. dos Santos, C.B. Jacobina, J.P.R.A. Mello, *Dynamic Voltage Restorer Based on Three-Phase Inverters Cascaded Through an Open-End Winding Transformer*, IEEE Transactions on Power Electronics, **31**, pp. 188–199, 2016.
2. *IEEE Recommended Practice for Monitoring Electric Power Quality*, IEEE Std. 1159–2009, 2009.
3. *IEEE Guide for Identifying and Improving Voltage Quality in Power Systems*, IEEE Std. 1250–2011, 2011.
4. A. Khoshkbar Sadigh, K.M. Smedley, *Fast and precise voltage sag detection method for dynamic voltage restorer (DVR) application*, Electric Power Systems Research, **130**, pp. 192–207, 2016.
5. M.E.C. Brito, L.R. Limongi, M.C. Cavalcanti, F.A.S. Neves, G.M.S. Azevedo, *A step-dynamic voltage regulator based on cascaded reduced-power series transformers*, Electric Power Systems Research, **108**, pp. 245–253, 2014.
6. A. Teke, L. Saribulut, M. Tumay, *A Novel Reference Signal Generation Method for Power-Quality Improvement of Unified Power-Quality Conditioner*, IEEETransactions on Power Delivery, **26**, pp. 2205–2214, 2011.
7. A. Teke, M.E. Meral, M.U. Cuma, M. Tümay, K.Ç. Bayindir, *OPEN unified power quality conditioner with control based on enhanced phase locked loop*, IET Generation, Transmission & Distribution, **7**, pp. 254–264, 2013.
8. S. Gupta, R.K. Tripathi, *Two-Area Power System Stability Improvement using a Robust Controller-based CSC-STATCOM,* Acta Polytechnica Hungarica, **11**, pp. 135–155, 2014.
9. M. Flitti, M.K. Fellah, M. Yaichi, M. Khatir, M.F. Benkhoris, *Control Design of Statcom Using Five Level Neutral Point Clamped Converter and Its Application to Reactive Power*, Rev. Roum. Sci. Techn. – Électrotechn. et Énerg., **59**, pp. 351–360, 2014.
10. L. Deng, J. Fei, C. Cai, *Global Fast Terminal Sliding Mode Control for an Active Power Filter Based on a Backstepping Design*, Rev. Roum. Sci. Techn.– Électrotechn. et Énerg., **61**, pp. 293–298, 2016.
11. C. Kumar, M.K. Mishra, *Predictive Voltage Control of Transformerless Dynamic Voltage Restorer*, IEEE Transactions on Industrial Electronics, **62**, pp. 2693–2697, 2015.
12. Y. Shuitao, L. Yang, W. Xiaorui, D. Gunasekaran, U. Karki, F.Z. Peng, *Modulation and Control of Transformerless UPFC,* IEEE Transactions on Power Electronics, **31**, pp. 1050–1063, 2016.
13. W.C. Lee, K.N. Sung, T.K. Lee, *Fast Detection Algorithm for Voltage Sags and Swells Based on Delta Square Operation for a Single-Phase Inverter System*, Journal of Electrical Engineering & Technology, **11**, pp. 157–166, 2016.
14. M.B. Latran, A. Teke, *A novel wavelet transform based voltage sag/swell detection algorithm*, International Journal of Electrical Power & Energy Systems, **71**, pp. 131–139, 2015.
15. M. Karimi-Ghartemani, *Linear and Pseudolinear Enhanced Phased-Locked Loop (EPLL) Structures*, IEEE Transactions on Industrial Electronics, **61**, pp. 1464–1474, 2014.
16. M. Karimi-Ghartemani, M.R. Iravani, F. Katiraei, *Extraction of signals for harmonics, reactive current and network-unbalance compensation*, IEE Proceedings – Generation, Transmission and Distribution, **152**, pp. 137–143, 2005.
17. Y. Han, M.Y. Luo, X. Zhao, J.M. Guerrero, L. Xu, *Comparative Performance Evaluation of Orthogonal-Signal-Generators-Based Single-Phase PLL Algorithms-A Survey*, IEEE Transactions on Power Electronics, **31**, pp. 3932–3944, 2016.
18. L. Asiminciaei, F. Blaabjerg, S. Hansen, *Detection is key – Harmonic detection methods for active power filter applications*, IEEE Industry Applications Magazine, **13**, pp. 22–33, Jul–Aug 2007.
19. A. Bhattacharya, C. Chakraborty, S. Bhattacharya, *Shunt Compensation*, IEEE Industrial Electronics Magazine, **3**, pp. 38–49, 2009.
20. M. Karimi-Ghartemani, M.R. Iravani, *A nonlinear adaptive filter for online signal analysis in power systems: Applications*, IEEE Transactions on Power Delivery, **17**, pp. 617–622, 2002.
21. M. Karimi-Ghartemani, H. Mokhtari, M.R. Iravani, M. Sedighy, *A signal processing system for extraction of harmonics and reactive current of single-phase systems*, IEEE Transactions on Power Delivery, **19**, pp. 979–986, 2004.
22. S. Gao, M. Barnes, *Phase-locked loop for AC systems: Analyses and comparisons*, Power Electronics, Machines and Drives, 6th IET International Conference on, 27–29 March 2012, pp. 1–6.
23. A.M. Rauf, V. Khadkikar, *An Enhanced Voltage Sag Compensation Scheme for Dynamic Voltage Restorer*, IEEE Transactions on Industrial Electronics, **62**, pp. 2683–2692, 2015.
24. A.K. Sadigh, K.M. Smedley, *Fast and precise voltage sag detection method for dynamic voltage restorer (DVR) application*, Electric Power Systems Research, **130**, pp. 192–207, 2016.
25. H.K. Al-Hadidi, A.M. Gole, D.A. Jacobson, *A novel configuration for a cascade inverter-based dynamic voltage restorer with reduced energy storage requirements*, IEEE Transactions on Power Delivery, **23**, pp. 881–888, 2008.
26. J. Wang, X. Hu, S. Chen, *Research on Detection Algorithm of Voltage Sag Characteristics*, Industrial Electronics and Applications (ICIEA), 7th IEEE Conference on, 2012, pp. 313–318.
27. J.Z. Yang, C.S. Yu, C.W. Liu, *A new method for power signal harmonic analysis*, IEEE Transactions on Power Delivery, **20**, pp. 1235–1239, 2005.
28. L Sarıbulut, A. Teke, M. Tümay, *Fundamentals and literature review of Fourier transform in power quality issues*, Journal of Electrical and Electronics Engineering Research, **5**, pp. 9–22, 2013.